Med. & Biol. Eng. & Comput., 1979, 17, 045–060

In vivo dielectric spectrometer

B. Singh* C. W. Smith R. Hughes**

Department of Electrical Engineering, University of Salford, Salford M5 4WT England

Royal Albert Edward Infirmary, Wigan, Lancashire, England

Abstract—*An instrument is described for measuring the relative permittivity and dielectric loss of body tissues and organs* in vivo, *over the frequency range 0·1 Hz to about 100 kHz. A voltage transient is applied by means of suitable electrodes and the resulting waveform is sampled, digitised and Fourier transformed using a microprocessor to give a spectrum in the frequency domain. The results show differences in relative permittivity and dielectric loss between different types of tissue. Much of the preliminary clinical work with this apparatus has been done using measurements on breast tumours.*

Keywords—*Biomedical dielectrics, Breast tumours, Fourier transforms,* In vivo *measurements*

1 Introduction

THE electrical properties of tissue and cell suspensions have been reviewed by SCHWAN (1957), who noted a wide frequency spectrum over which dispersion regions can be expected. It is evident from his results that the dielectric properties of these materials show a pronounced dispersion at low frequencies. The values of the relative permittivity at low frequencies are also very high, being often in excess of 10^6. SCHWAN (1957) shows a typical example of the dependence of relative permittivity on frequency for such materials. The three dispersions are classified as α, β and γ dispersion regions, respectively.

The dispersions at higher frequencies are explained on the basis of some generalised formulations given by SCHWAN (1957). However, the very high values of relative permittivity at low frequencies (0·01 to 100 Hz.) remain unexplained. This is mainly due to the difficulty of making precise measurements because of instrument limitations and because of the way that such measurements are made.

It is a reasonable assumption that electrical properties of most living tissues will change when they are taken out of their natural environment. The dielectric properties of dead tissues will show a greater change even, hence, to obtain a reasonable assessment of these values at low frequencies, the measurements would have to be made *in vivo* and in a reasonably short time so as to prevent any semi-permanent changes or 'fixation of tissues' as a result of the externally applied field. Existing methods of measurement are based mostly on impedance bridges. These prove to be inadequate at frequencies below 100 Hz due to problems such as noise, instability, electrode polarisation and the time required to obtain the balance conditions. Most impedance bridges operate from a mains power supply; furthermore, they yield the impedance values only at discrete frequencies. This is not suitable for *in vivo* measurements where physiological changes may be expected to occur between individual readings. The most reasonable possibility is offered by some kind of dielectric spectrometer, which could have that part attached to the subject operated from batteries instead of the mains supplies.

This report describes the development and construction of such an instrument. Since tissues such as blood, muscle, skin and fat are composed of comparatively large molecules and include much membrane structure, the Maxwell–Wagner effect and effects due to membrane capacitance also need to be considered.

2 Measuring technique

2.1 *Basic principles*

For a capacitor having unity vacuum capacitance, but filled with the material to be measured as the dielectric, the current response $i(t)$ to a unit step voltage is connected with the complex relative permittivity by the Fourier transform (HYDE, 1970)

$$\hat{\varepsilon}(\omega) = \varepsilon'(\omega) - j\varepsilon''(\omega) = \int_0^\infty i(t) \exp(-j\omega t)\, dt \quad (1)$$

*Now at the Department of Electrical Engineering, University of Sulymania, Sulymania, Iraq

**Now at the Department of Surgery, University Hospital of South Manchester, Manchester M20 8LR, England

First received 5th December 1977 and in final form 10th May 1978

0140–0118/79/010045+016 $01·50/0

where ω is the angular frequency and $\varepsilon'(\omega)$ and $\varepsilon''(\omega)$ are the real and imaginary parts of the complex relative permittivity, respectively. A major practical difficulty in using this method to obtain steady-state information arises from the problem of truncation. Clearly, any set of experimental data can only cover a finite range in time, and errors will, therefore, arise owing to the cutting-off of the Fourier integral at both small and large values of the time variable t. The magnitude of such errors will depend on the time range of available data, the value of ω in relation to the minimum and maximum values of t and on the form of $i(t)$ itself. It has been noted that biological materials exhibit relaxation phenomena which are fairly well defined.

in the problem of excessive currents passing in biological materials in general and especially in the case of human subjects where safety considerations are involved. To overcome this difficulty, a double polarity pulse is employed. Instead of the sample being used as the only capacitor, a second and variable capacitor is connected in series with the sample, as shown in Fig. 1.

The signal is obtained from the junction of the two capacitors; thus the resultant unbalance charging current is measured. If the value of the air capacitor is adjusted to a value close to the value of the sample capacitor, the resultant unbalance current $i(t)$ can be reduced considerably. This, however, does not change the shape of the transient $i(t)$ because

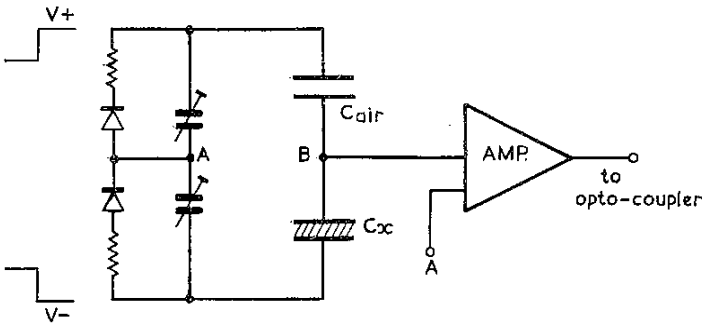

Fig. 1 Method used to apply pulse to specimen C_x and to compensate for transient current

A relaxation system can be described as one whose response to a step-function stimulus is a monotonic decrease towards zero. In the case of dielectric materials, a voltage step applied to the specimen results in a monotonically decaying current $i(t)$. To obtain an accurate value of $\hat{\varepsilon}(\omega)$ using eqn. 1 it is necessary to collect $i(t)$ data over as wide a range of times as possible. The form of the curve $i(t)$ is, in general, an exponential decay, but if there is a distribution of relaxation times this curve will be a combination of more than one exponential. In the following Sections a practical method for deriving complex dielectric constant values with reasonable accuracy from such $i(t)$ data is described.

Ordinarily, it would be sufficient to apply the step stimulus direct to the sample, but this may result

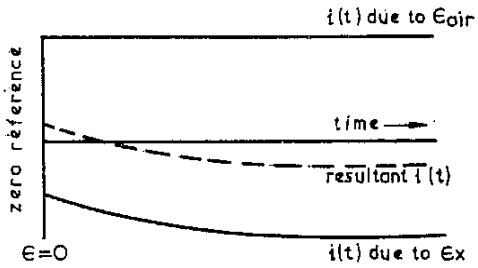

Fig. 2 Combined effects of C_{air} and C_x

the air capacitor is an ideal capacitor with no leakage and it charges up instantaneously. This state of affairs can best be illustrated by the diagram of charging currents shown in Fig. 2.

2.2 *Theory of Fourier transform analysis applied to a step response*

Consider that the sample is equivalent to a generalised admittance Y, so that

$$Y(\omega) = G(\omega) + j\omega C(\omega) \quad . \quad . \quad . \quad . \quad . \quad (2)$$

where $G(\omega)$ is the frequency dependent conductance and $C(\omega)$ the frequency dependent capacitance. Consider that the admittance is driven by a voltage $U(t)$ and the resulting output transient is $i(t)$. Application of the Laplace transform yields

$$Li(t) = Y(\omega)\, LU(t) \quad . \quad . \quad . \quad . \quad . \quad . \quad (3)$$

Now, in the case of a step voltage

$$U(t) = 0 \qquad \text{when } t \leqslant 0$$

and

$$U(t) = V \qquad \text{when } t > 0$$

then

$$LU(t) = V/j\omega \quad . \quad . \quad . \quad . \quad . \quad . \quad . \quad . \quad (4)$$

therefore

$$Y(\omega) = \frac{j\omega}{V} \int_0^\infty i(t) \exp(j\omega t)\, dt \quad . \quad . \quad . \quad (5)$$

is obtained by equating real and imaginary parts

$$G(\omega) = \frac{\omega}{V} \int_0^\infty i(t) \sin(\omega t)\, dt \quad . \quad . \quad . \quad . \quad (6)$$

$$C(\omega) = \frac{1}{V} \int_0^\infty i(t) \cos(\omega t)\, dt \quad . \quad . \quad . \quad . \quad (7)$$

To eqns. 6 and 7 must be added the steady values of conductance G_0 and the high-frequency capacitance C_∞, respectively to obtain correct values of these quantities, therefore

$$G_T(\omega) = G_0 + \frac{\omega}{V} \int_0^\infty i(t) \sin(\omega t)\, dt \quad . \quad . \quad (8)$$

$$C_T(\omega) = C_\infty + \frac{1}{V} \int_0^\infty i(t) \cos(\omega t)\, dt \quad . \quad . \quad (9)$$

In practice, however, the integrals 8 and 9 have to be truncated after a reasonable period of time.

2.3 *Solution of Fourier integrals using a straight-line approximation*

Let p_1 and p_2 be two points so that $p_1 = i(t_1)$ and $p_2 = i(t_2)$, where t_1 and t_2 are the two consecutive times starting from the time of the first sample t_0, which is taken as the zero time. If the interval $(t_2 - t_1)$ is small, then the function $i(t)$ between t_1 and t_2 can be considered to be a straight line. The slope of this line will be given by

$$m = (p_2 - p_1)/(t_2 - t_1) \quad . \quad . \quad . \quad . \quad . \quad . \quad . \quad (10)$$

and the intercept c is given by

$$c = p_1 - t_1(p_2 - p_1)/(t_2 - t_1) \quad . \quad . \quad . \quad . \quad (11)$$

therefore

$$i(t) = mt + c \quad . \quad . \quad . \quad . \quad . \quad . \quad . \quad . \quad . \quad (12)$$

between the points p_1 and p_2.
The Fourier integrals, therefore, become

$$\int_{t_1}^{t_2} i(t) \sin(\omega t) = \int_{t_1}^{t_2} (c + mt) \sin(\omega t)\, dt \quad . \quad (13)$$

and

$$\int_{t_1}^{t_2} i(t) \cos(\omega t) = \int_{t_1}^{t_2} (c + mt) \cos(\omega t)\, dt \quad . \quad (14)$$

Integrating eqn. 23 by parts yields

$$\int_{t_1}^{t_2} i(t) \sin(\omega t)\, dt = \frac{mt \sin(\omega t)}{\omega} + \frac{m \sin(\omega t)}{\omega^2} - \frac{c \cos(\omega t)}{\omega} \int_{t_1}^{t_2} \quad . \quad . \quad . \quad (15)$$

Inserting limits of integration and substituting the values for m and c in eqn. 15 gives

$$\int_{t_1}^{t_2} i(t) \sin(\omega t)\, dt = \frac{p_2 - p_1}{(t_2 - t_1)\omega^2} [\sin(\omega t_2) - \sin(\omega t_1)] + \frac{1}{\omega} [p_1 \cos(\omega t_1) - p_2 \cos(\omega t_2)] \quad . \quad (16)$$

Similarly, from eqn. 14, we obtain

$$\int_{t_1}^{t_2} i(t) \cos(\omega t)\, dt = \frac{p_2 - p_1}{(t_2 - t_1)\omega^2} [\cos(\omega t_2) - \cos(\omega t_1)] + \frac{1}{\omega} [p_2 \sin(\omega t_2) - p_1 \sin(\omega t_1)] \quad . \quad (17)$$

Eqns. 16 and 17, when summed over all the intervals of time, yield the required values of $G_T(\omega)$ and $C_T(\omega)$ from which the complex dielectric constant can be derived. The loss angle is given by

$$\tan \phi = G(\omega)/\omega C(\omega) \quad . \quad . \quad . \quad . \quad . \quad . \quad . \quad (18)$$

So long as the straight line approximation applies between any two consecutive sampling times, the width of the sampling interval is unimportant. With this technique, therefore, both simplicity and the saving of data storage space is achieved.

In the limiting case, when t_1 and t_2 are close together and ω is large, the first term on the right hand side of eqn. 16 is very small compared with the second term, and the second term becomes $\Delta V/\omega$ where ΔV is the difference in voltages at the two points p_1 and p_2. Therefore

$$\int_{t_1}^{t_2} i(t) \sin(\omega t)\, dt = \Delta V/\omega \quad . \quad . \quad . \quad . \quad . \quad (19)$$

If $\omega = 1/t$, then $\varepsilon''(\omega) = Bti(t)$, B being a constant depending on the amplifier gain, electrode size and the value of voltage step. This last expression gives the approximate value of $\varepsilon''(\omega) = (2{\cdot}1) \times t \times i(t)$ calculated on the basis of just two points and it

compares well with those of HAMON (1952) and HYDE (1970) who obtain $\varepsilon''(\omega) = (1{\cdot}59) \times t \times i(t)$ and $\varepsilon''(\omega) = (\pi/2) \times t_1 \times i(t_1)$, respectively, for approximate value of $\varepsilon''(\omega)$ derived from just two points on the output current transient.

HYDE (1970) derives the accuracy of the approximate transforms on the basis that any approximate transform which deals successfully with Debye relaxation can be shown to be at least as good for any other relaxation process. The accuracy of the derived transforms used with this device has been checked on the basis of the above statement.

3 Description of apparatus

A block diagram of the whole system is shown in Fig. 3*a* and 3*b* and the main units are described in the following Sections.

The cycle of operation of the apparatus is initiated by pressing the switch *S*. This generates the voltage transient applied to the subject or tissue sample and releases the PAUSE, enabling the microprocessor to carry out its instructions.

The current resulting from the voltage transient is fed by way of a capacitor bridge to a high input impedance, low offset current amplifier and after to an optocoupler providing isolation from the mains operated equipment, it is sampled and digitised in the analogue-digital convertor under the control of the microprocessor. The required number of samples are obtained and stored in specified memory locations from where they are available for transforming to the frequency domain.

3.1 *Step generator*

The circuit diagram of the step generator is given in Fig. 4. Voltage transients with amplitudes ranging from $\pm 0{\cdot}75$ V to ± 45 V can be generated using convntionael dry batteries of layer construction as they provide good voltage stability. Resistors R_1 and R_2 are selected carbon resistors of nominal 5% accuracy and each is 100 Ω in value. These two resistors are specially selected for a match because they act as the potential divider for the generation of the bipolar step waveform. D_1 and D_2 are two germanium diodes: D_1 starts conducting as soon as the voltage is applied to R_1 and the small voltage developed across D_1 can be used for triggering the rest of the system. The diode D_2 is added for symmetry. Diodes are used instead of resistors, because they provide a triggering signal whose magnitude is largely independent of the magnitude of the step voltage being generated. The two small adjustable air capacitors C_1 and C_2 are added to cancel out any capacitance unbalance that will result in asymmetry between the two polarities of the step. An electronically controlled switch completes the circuit. It uses a 741J Dual Schmitt to trigger the transistor switch, thus giving a pulse

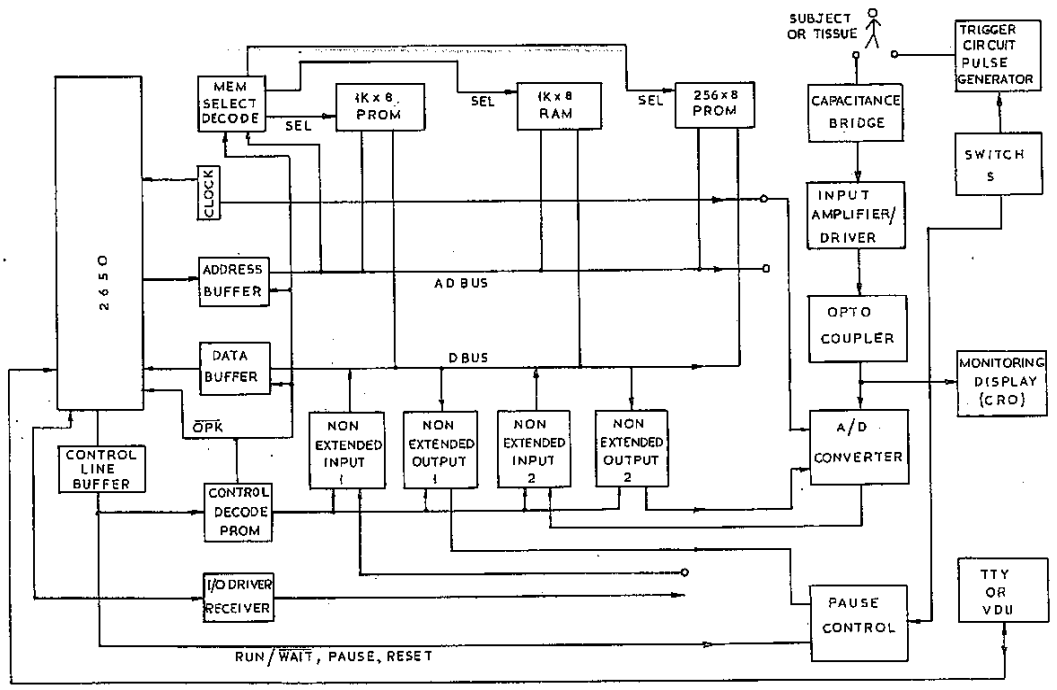

Fig. 3A Dielectric spectrometer

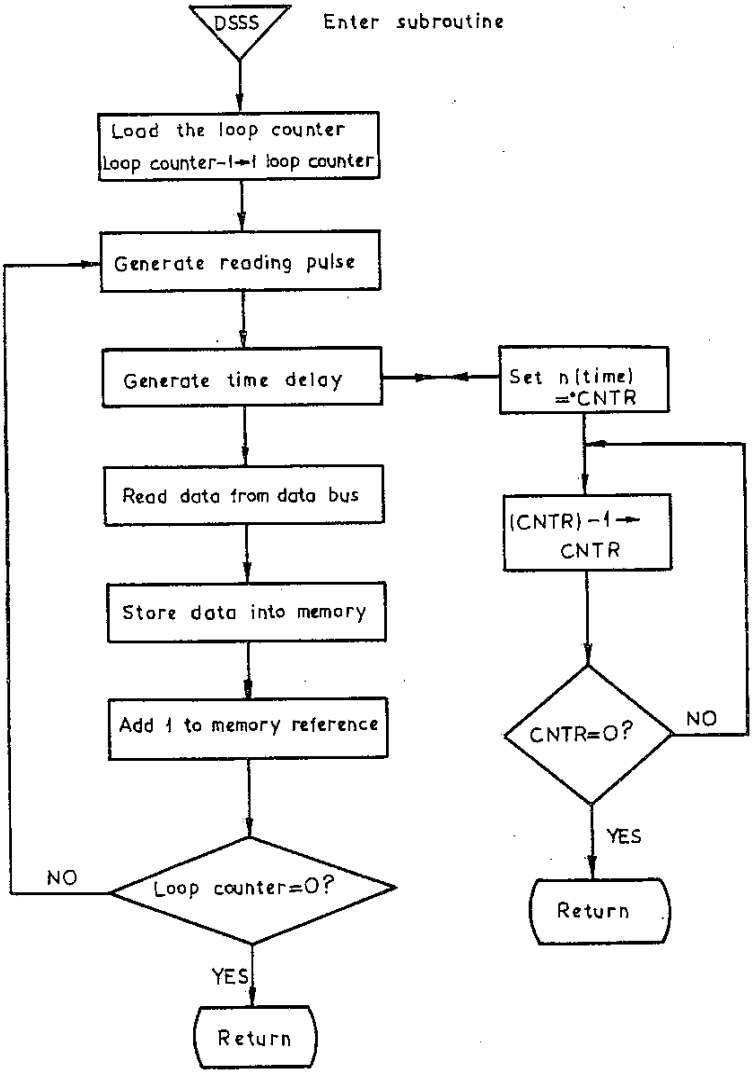

Fig. 3B Flow chart for data sampling and storage subroutine (d.s.s.s.)

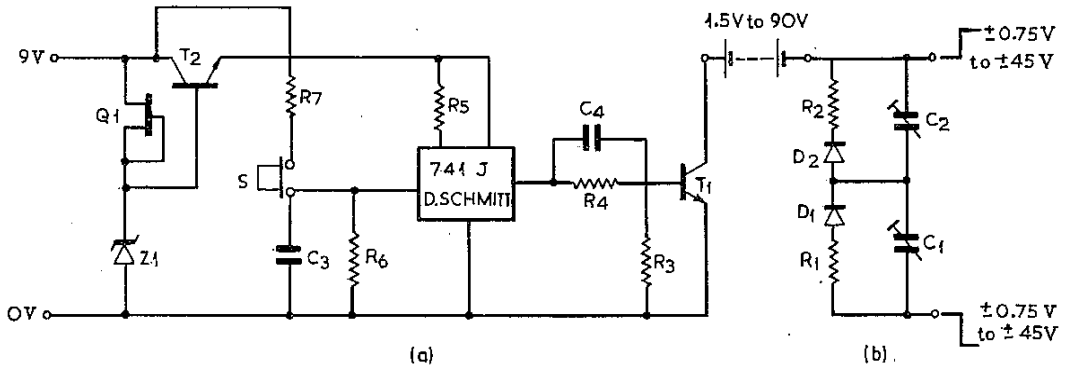

Fig. 4 Double polarity pulse generator and triggering circuit

free from contact bounce and other defects and having a rise time of 50 ns. Any contact bounce arising from the mechanical push button switch S is compensated by the small capacitor C_3. Moreover, since the rise time of the leading edge of the pulse is very small (50 ns) compared with time t_0 for the first sampling, any raggedness on the leading edge of the pulse does not affect the results. This circuit performed very satisfactorily producing steps of opposite polarity simultaneously and having equal and constant amplitude for periods up to at least 10 min.

3.2 *Capacitance bridge*

Between the step generator and the amplifier is the circuit shown in Fig. 1, which is a close approximation to a capacitance bridge. C_{air} is the reference air capacitor; this is adjusted to obtain the signal in the required form, which is: decreasing in magnitude and negative to the zero reference of the circuit at all times. This last condition is only needed because of the way the analogue-digital convertor operates. The differential signal between points A and B in Fig. 1 is fed to the amplifier.

3.3 *Amplifier*

The amplifier was constructed from an f.e.t. input operational amplifier (μA741) having a high input impedance ($10^{12}\ \Omega$), a low input offset current (40 pA) and a low input bias current (150 pA maximum). It has a frequency bandwidth product of 100 kHz at an open-loop voltage gain of about 100. However, this input stage was operated at unity gain, thus ensuring an even better bandwidth. The signal amplification was obtained from the second stage amplifier consisting of μA709 operational amplifier. Overall, it was possible to obtain a gain of 4 dB and a frequency range from 0 to 100 kHz. The rise time of the instrument was better than 500ns. The details of this circuit are given in Fig. 5. Resistor R_{10} is adjustable to effect the gain control. Most of the common mode rejection is obtained by carefully matching the ratio of resistors $R_3/R_1 = (R_4 + R_5)/R_2$. This is attained by adjusting the preset trimmer R_5. The resulting common mode rejection ratio at the first stage of the amplifier is thus better than 80 dB. A voltage offset null resistor is also provided in the first stage (R_{16}) but this gives only a limited dynamic offset range. The instrument is meant to be used on samples which have a considerable leakage current, the input current swing can be very asymmetrical. To accommodate these rather large swings in the input signal, another voltage offset null circuit is included. It consists of resistors R_{12} and R_{13}, where R_{13} serves as the potential divider and the resistor R_{12} limits the input current at the inverting input end of the input amplifier which is at vitural earth. With the help of this arrangement it is possible to accommodate input signals up to the full output swing

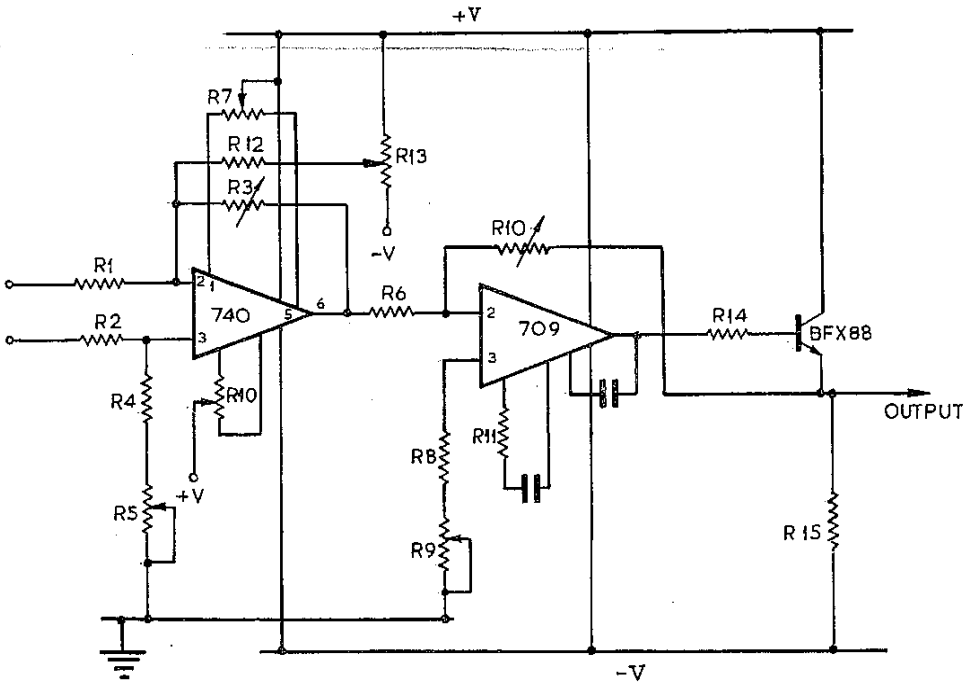

Fig. 5 Amplifier circuit: resistors R_3 and R_5 are preset, R_{10} is a gain control

range of the amplifier (the supply rail voltages) without clipping.

The output of the amplifier is fed through an optocoupler (Fig. 6) providing electrical isolation from the mains powered circuits which followed. The output from the optocoupler is at present fed to a storage oscilloscope and to the analogue-digital convertor.

3.4 *Analogue-digital convertor*

A Teledyne Philbrick 4114 8-bit analogue-digital convertor is used. It is operated in parallel mode and is controlled by the microprocessor. It requires about 45 μs for the conversion and the linearity is $\pm 1/2$ LSB (least significant bit) at 25°C maximum. The microprocessor's internal clock is used for the conversion and the reference voltage is also that provided internally. Fig. 7 is the timing diagram for the conversion. The reset pulse is provided by the microprocessor. This is obtained by sending a logic zero bit (low) on the data bus which is normally kept at logic one (high). This instruction takes 2 μs (two clock periods of the microprocessor clock) and is more than sufficient to reset the a.d. convertor which only needs a 0·1 μs wide resetting pulse. The 8-bits representing the value of $i(t)$ (Fig. 2) at that moment are directly stored into the microprocessor memory. The a.d. convertor is operated in the single conversion mode, therefore until the next instruction for conversion arrives, the previous status persists.

When $i(t)$ is converted to digital form, it is represented as a finite integer number in binary form. With an 8-bit a.d. convertor, the maximum value of this number is $2^8-1 = 255$. Since the convertor has an accuracy of $\pm 0{\cdot}5$ LSB, at full range, the accuracy of the binary number will be of the order of $\pm 0{\cdot}2\%$. The output from the microprocessor is in hexadecimal form which results in an accuracy of $\pm 3\%$. The rounding-off errors in the

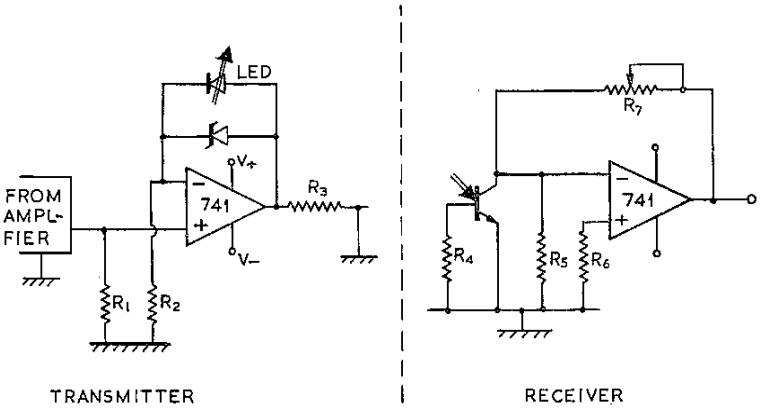

Fig. 6 Optocoupler to provide isolation of the patient circuits from the mains-powered microprocessor

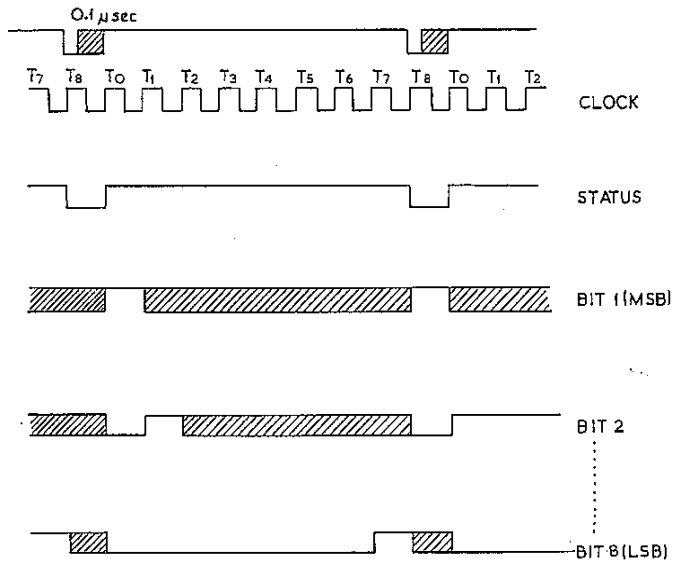

Fig. 7 Timing diagram for the analogue-digital convertor

following calculations are very small (half a digit in 16 digit number representation) and therefore the overall accuracy is limited only by the output limitation of the microprocessor and hence is of the order of $\pm 3\%$. The minimum measurable level of pemittivity is limited by the voltage resolution of the a.d. convertor. For applied voltage steps of 10 V, the minimum resolution is $10/(2^8-1) = 4$ mV. With the amplifier having a voltage gain of 100, this corresponds with an input voltage signal of 40 μV and an unbalance between C_{air} and C_x of 1 part in $2 \cdot 5 \times 10^4$.

4 Method of operation

4.1 *Microprocessor*

Since this work was commenced there has been a great development in microprocessors, so that it was not found necessary to develop specific circuits to perform the Fourier transform (Section 2). The microprocessor is used both to control the measuring circuit and to compute the values of complex dielectric constant from the sampled $i(t)$ data. A Signetics 2650 8-bit parallel microprocessor was used. This processor includes facilities of parallel and serial input/output. The address and data busbars are tristate, and thus the machine can be very easily interfaced with other circuits. This general purpose processor can perform any data manipulations through the execution of a stored sequence of machine coded instructions. It has a total of seven general purpose registers arranged in two banks and can address up to 32786 bytes of memory, in four pages of 8192 bytes each. Thus, it can handle a large number of sequential instructions. The basic cycle time is 1 μs and the most complicated three byte direct instruction will not take more than 9·6 μs to execute. Memory and input/output interfaces are asynchronous so that direct memory access (d.m.a.) and multiprocessor operations are possible.

4.2 *Synchronisation*

The program in the programmable read only memory (p.r.o.m.) of the microprocessor controls the synchronisation of the whole equipment. The processor is started by the GO command instruction. A square pulse is obtained from the output port of the central processor unit (c.p.u.) and is fed into a differentiating circuit (Fig. 8) which produces the reset signal for the dual flip-flop (7474). When the Q output of the flip-flop is driven to logic zero, the PAUSE condition of the c.p.u. is driven to low, which enters it into a WAIT state, when it stops executing the instructions. This also means that the Q output of the flip-flop is high and that the transistor T_2 is conducting, which results in the light emitting diode being lit. When the switch S is closed, it sets the 7474 flip-flop and its Q output goes high, which results in the PAUSE being released so that the c.p.u. carries on with the execution of the next set of instructions; the switch S also operates the pulse generator (Fig. 4). As soon as the switch S is closed, a pulse is applied to the trigger circuit, output analogue generates the double polarity pulse and the resulting signal is fed into the a.d. convertor which then receives the instruction from the c.p.u. for

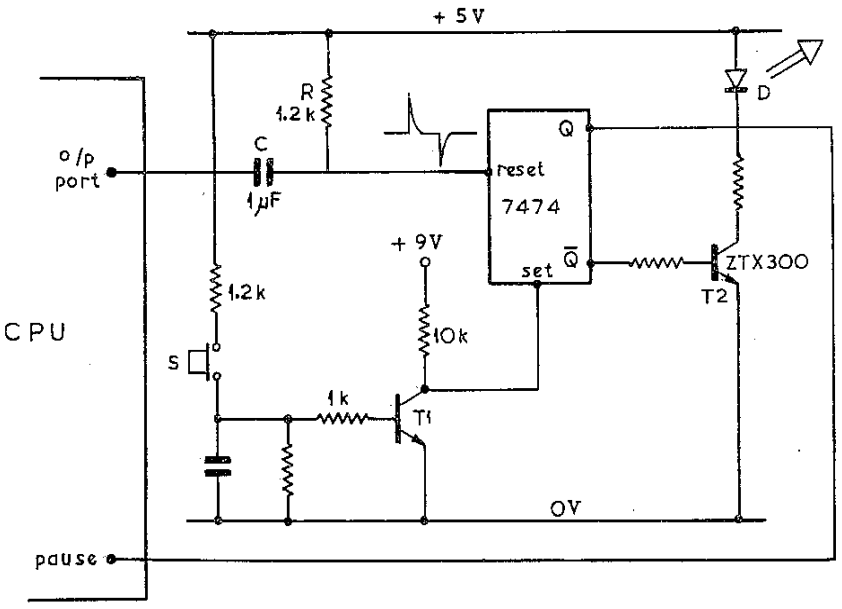

Fig. 8 Delay generator and synchronising circuit

conversion and storage of the digital data. The eight binary bits representing the voltage at that instant are stored into a predetermined memory location of the r.a.m. (random access memory). The next instruction adds one to the memory reference instruction so that the next data value is stored in the successive memory location. The number of samples to be stored is determined by presetting a register to that number to form a loop counter. The sampling rate is determined by setting loop counters in the delay routines to an appropriate value. There is a limit to the minimum sampling time available due to the finite number of instructions required to perform the sampling of the data. At present, the minimum sampling interval is 150 μs. This is equivalent to a sampling frequency of 60 kHz. The corresponding Nyquist frequency will be 30 kHz. The limitation to the lowest frequency available is the stability of the batteries from which the voltage step is derived. A range of frequencies varying from 0·01 Hz to 30 kHz is available at present, and this includes the α-dispersion region (SCHWAN, 1957).

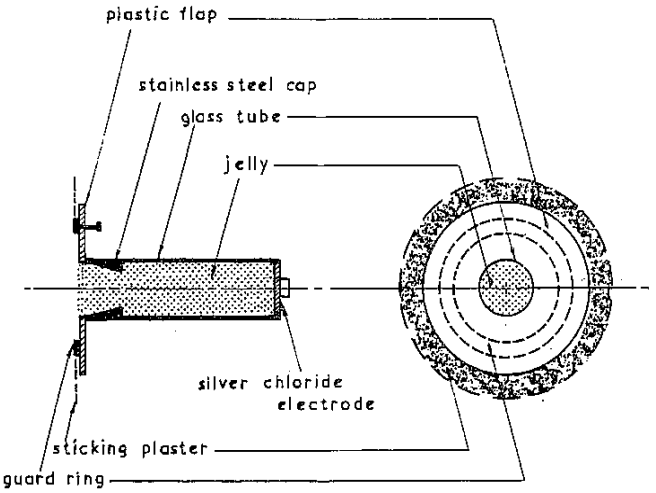

Fig. 9 Jelly electrode

4.3 *Experimental details*

The capacitor C_x in Fig. 1 is replaced by the sample which may be a piece of excised tissue, or a patient or subject, to which two specially prepared jelly-type silver/silver-chloride electrodes are applied. Details of the electrodes are given in Section 4.4. On the application of the double polarity voltage step to the sample, an output current transient exponentially decaying with time can be observed on a storage oscilloscope. The offset null facility of the amplifier circuit is adjusted to make the entire output transient negative to the zero reference voltage (Fig. 2). This is necessary because of the way in which digitisation is carried out at present. The form of the transient gives an apparent value for the time constant and hence the characteristic frequency of relaxation of the system. This information is required for setting up the sampling rates. The other data, such as the electrode dimensions and the value of C_{air} (Fig. 1), are also inserted at this stage. Having set the apparatus thus, the loop counter register in the microprocessor is loaded with the appropriate sampling frequency and the microprocessor is started. The first few instructions generate a PAUSE condition and a PAUSE ON warning indication. As soon as the subject or other experimental arrangements are ready, the switch S is operated. This brings the microprocessor into operation which then starts executing the rest of its programmed instructions. At the same time the double polarity pulse is applied to the subject or sample. From the instant the processor is started, it takes about 10 μs for sampling to commence. The rise time of the amplifier is 0·5 μs, so that the pulse is well clear of any initial transients by the time that sampling starts. Since the sampling rate and the number of samples is preset, the microprocessor stops itself after the required number of samples have been obtained and stored into the specified

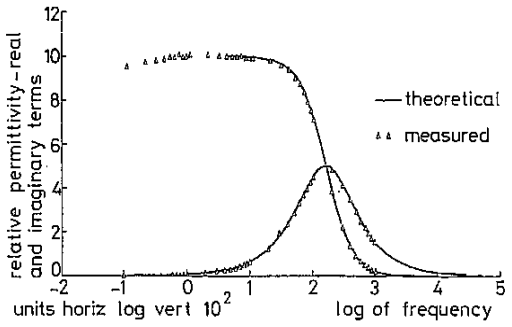

Fig. 10 Single relaxation-time lumped-circuit response: curves are calculated from component values, points are measured values

memory locations. The results are at once available on the visual display unit (v.d.u.) screen or can be obtained on a teletype or be punched on paper tape.

4.4 *Electrodes*

One of the major difficulties in making measurements on biological materials is that of electrode polarisation due to the differential mobility of electronic and ionic charge carriers at the interface between the sample and the electrode. This problem is even more acute in the case of low-frequency measurements, especially those tending towards zero frequency. In the case of a.c. measurements, dry electrodes and jelly-type electrodes were found to be satisfactory for certain specific cases. With the present instrument the applied transient is effectively d.c., and hence the electrode problem warranted special investigation.

To establish the types of electrodes which could be used successfully, a variety of electrodes were tried on a number of different types of samples. The quality of the response of these electrodes was quite obvious from the trace as seen on the monitor oscilloscope. The electrodes studied this way included the commonly used e.c.g. jelly electrodes, stainless-steel disc electrodes, 'Mylar' silver-chloride-coated band electrodes, stainless-steel hypodermic needles of varying sizes and tungsten microelectrodes. It was found that the e.c.g. type of jelly electrodes, which contained the electrode jelly in a foam-plastic sponge, were very satisfactory for *in vivo* measurements. On the other hand, for measurements on excised tissues, the tungsten microelectrodes were found to be satisfactory in respect of obtaining reproducible results. Although it was possible to define the active surface area of the e.c.g. electrodes without much difficulty if a specially mounted guard ring was used with these electrodes (Fig. 9), this was not the case with the subcutaneous needle-type electrodes. Since the effective area of the electrodes is needed for the calculation unless the VAN DER PAUW (1958) method is used, the needle-type electrodes did not give absolute values for the complex dielectric constant of the sample. The band electrodes were found to be unsatisfactory for three reasons; first, they did not make a good enough contact with the whole circumference of the limb; secondly they tended to produce a slight occlusion of the limb resulting in significant and measurable, although small, changes in the peripheral blood flow; thirdly, they of necessity measure only very large sections of the limbs and were difficult to fix in any symmetrical configuration, such as on the breasts. In general, the e.c.g. type electrodes were found to be the most satisfactory,

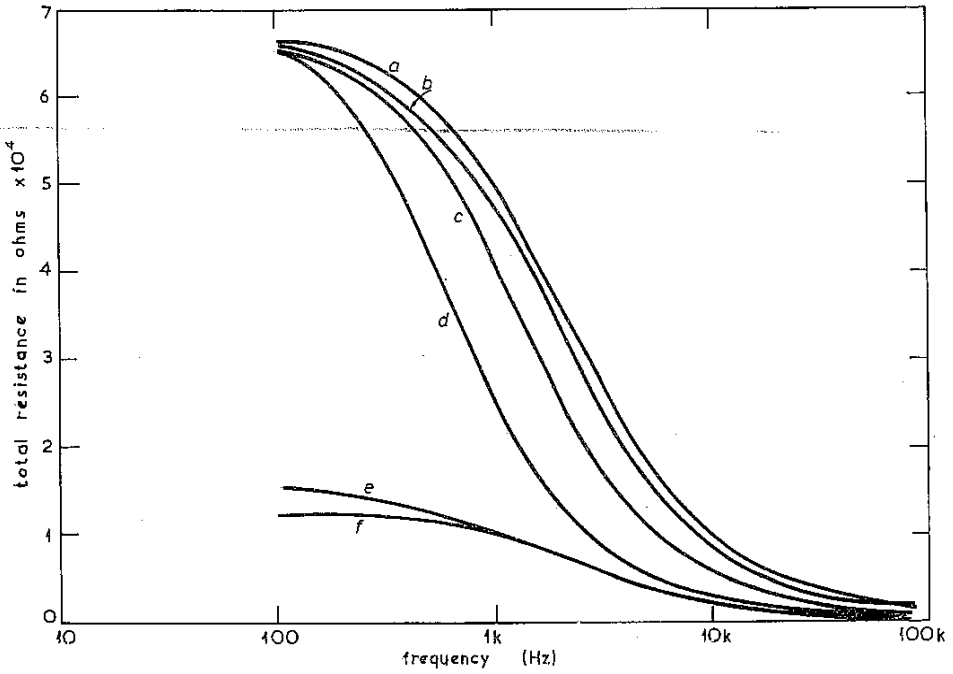

Fig. 11 Total impedance of various tissues measured at discrete frequencies, using surface electrodes. Curves a *and* b *are for normal breasts, curve* c *is for a breast with a malignant tumour, curve* d *is for a breast with a benign tumour using hypodermic needle, curve* e *for a normal breast and curve* f *for a breast with a benign tumour*

because it was possible to reduce the polarisation effects at the skin interface as described below.

When a metallic electrode comes in contact with an electrolyte various charge migrations take place which eventually reach equilibrium with the formation of an electrical or Helmholtz double layer. Once equilibrium has been reached (usually within a fraction of a second), there is no net outflow of charge from the interface double layer.

In the context of the present measurements, the electrodes are subject to the application of the voltage pulse. This results in polarisation of the electrode/electrolyte interface, because any passage of current through such an interface has to be

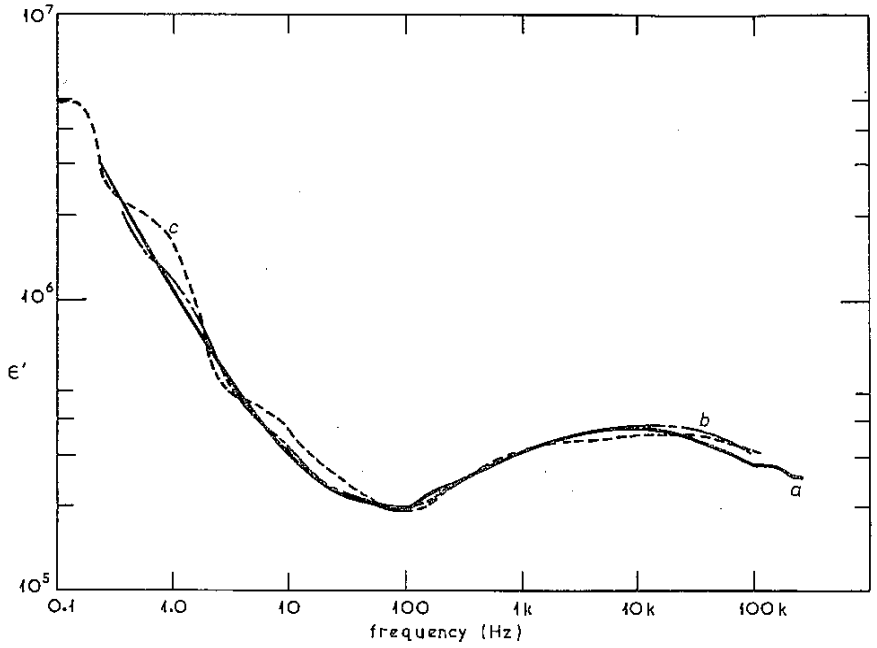

Fig. 12 Measurements with the dielectric spectrometer on normal arms (curves a and b) and on a normal arm with occluded circulation (curve c)

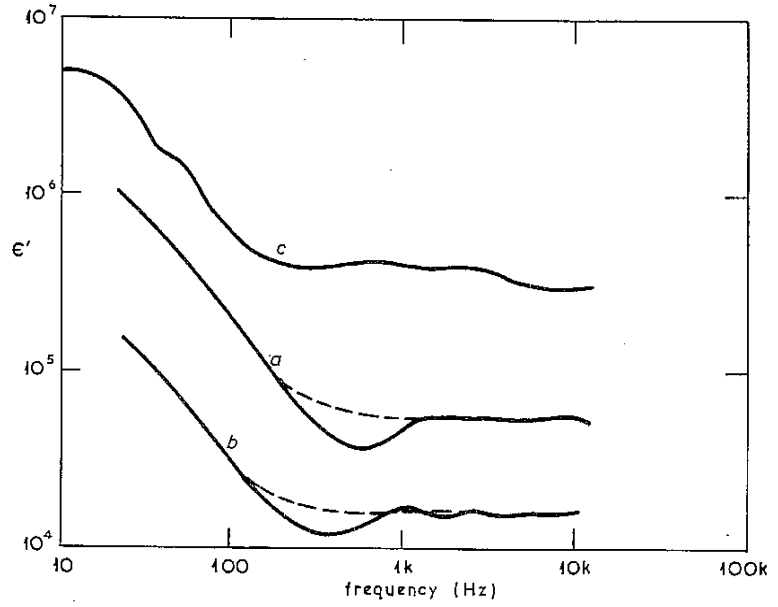

Fig. 13 Dielectric spectra for fresh venous (heparinised) blood (curve a), for r.b.c. enriched blood (curve b) and for clotted blood (curve c). The dotted sections represent a fitted Debye relaxation curve

sustained by a net reaction at the anode or the cathode. This will amount to the presence of a net potential over and above the equilibrium potential at each electrode. Let this potential be called the polarisation potential and be denoted by V_p. It is composed of three different components, thus

$$V_p = V_0 + V_c + V_a \quad . \quad . \quad . \quad . \quad . \quad . \quad . \quad (20)$$

where V_0 is the ohmic potential, V_c is the concentration potential and V_a is the activation potential.

Of these three components, the concentration potential V_c is the principle contributor to the value of V_p (KOLTHOFF and LINGANE, 1952). The reason for this potential is the mass-transfer processes of migration, diffusion and convection. A detailed

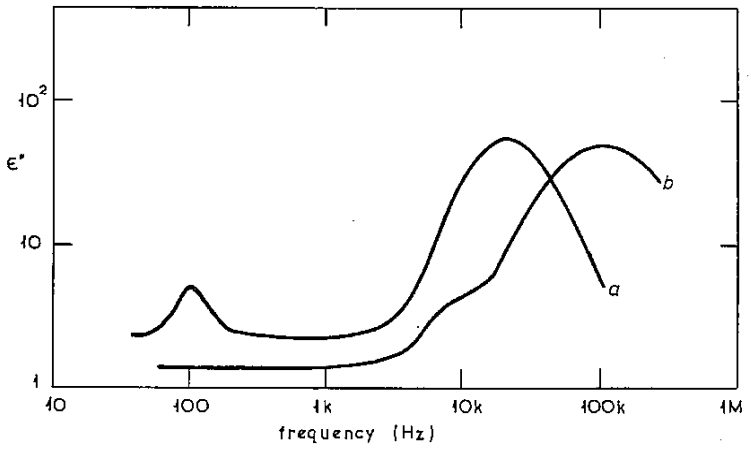

Fig. 14 Effect of two relaxation times in the specimen is shown for a two time constant Debye lumped-circuit (curve a) and for a piece of excised breast fatty tissue (curve b)

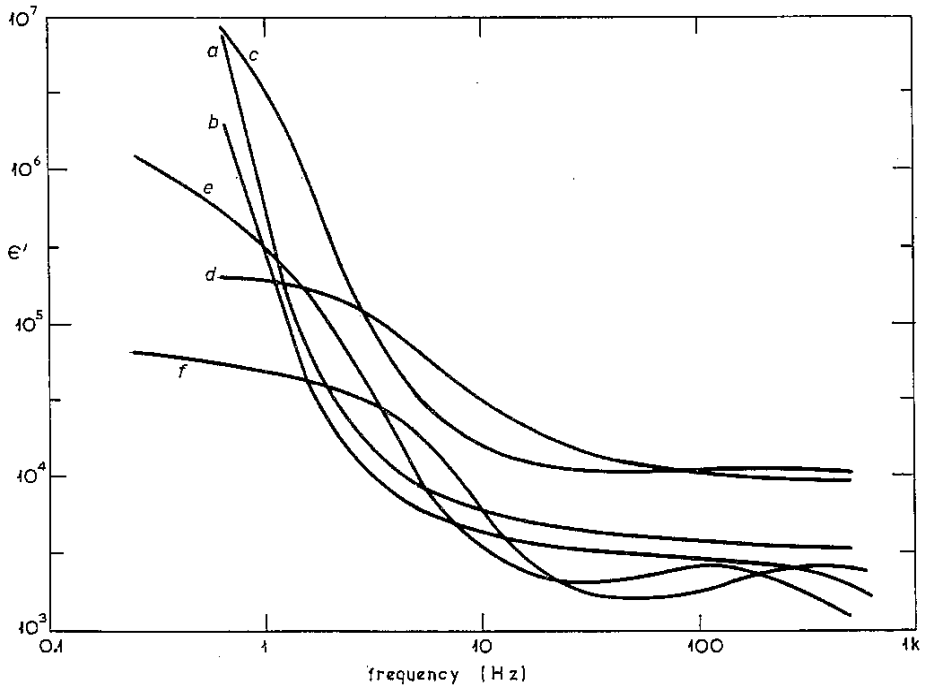

Fig. 15 In vivo *dielectric spectra*

Externally applied electrodes: a *Normal breast,* b *Normal breast, different subject,* c *Breast with malignant tumour,* d *Breast with benign tumour,* e *Extensor muscle origin, Hypodermic electrodes:* f*Normal breast*

treatment of these processes has been given by DELAHAY (1954). The following paragraphs give a brief description of these processes as applicable to a simplified model of the electrodes.

Consider an insulating tube (long compared with its diameter) which is filled with an electrode jelly of ionic diffusion constant D and is covered on one end with a silver-chloride-coated electrode, while at the other end the jelly makes contact with the sample. On the application of a potential difference, a current will start flowing through the jelly proportional to the ion mobility in the jelly and the reaction rate at the metal electrode. Since the interface between the chloride ions in the jelly and the metal plate is silver chloride, there will be no charge accumulation. On the other hand, if any other ions which do not react with the silver chloride are extracted from the sample and travel through the column of jelly to arrive at the metal surface, then this will produce a polarisation potential. If the column of jelly is made long enough so that ions from the sample do not have time to reach the metal surface before the end of the experiment, then these polarisation effects will be avoided.

5 Experimental results

The accuracy of the equipment was assessed by making measurements on a single time constant Debye lumped circuit. This circuit contained a d.c. conductance parameter and a high-frequency capacitance parameter so that it was a close approximation to the actual tissue samples. The values of the test circuit components were chosen after some preliminary measurements on tissues and subjects. The continuous curves in Fig. 10 are calculated for the values of the Debye lumped circuit components and the measured values are superimposed. As seen, the measured values lie close to the theoretical curves and although the measured values show some departure from the calculated values at the low-frequency end of the spectrum, at higher frequencies the values agree well with the calculated values. This shows that the instrument measures the relative permittivity represented by these discrete components with $\pm 3\%$ accuracy over the frequency range 0·1 Hz to 10 kHz.

5.1 *Measurements on biological materials*

Measurements were made on biopsy and post-mortem tissue samples. The instrument was used to make a number of *in vivo* measurements on different parts of human bodies. The most significant results were obtained from female breasts some of which contained tumours. These measurements were complemented by impedance measurements at discrete frequencies using an impedance bridge (Fig. 11). In the early stages of the project, preserved tissues were measured. It was then realised that the

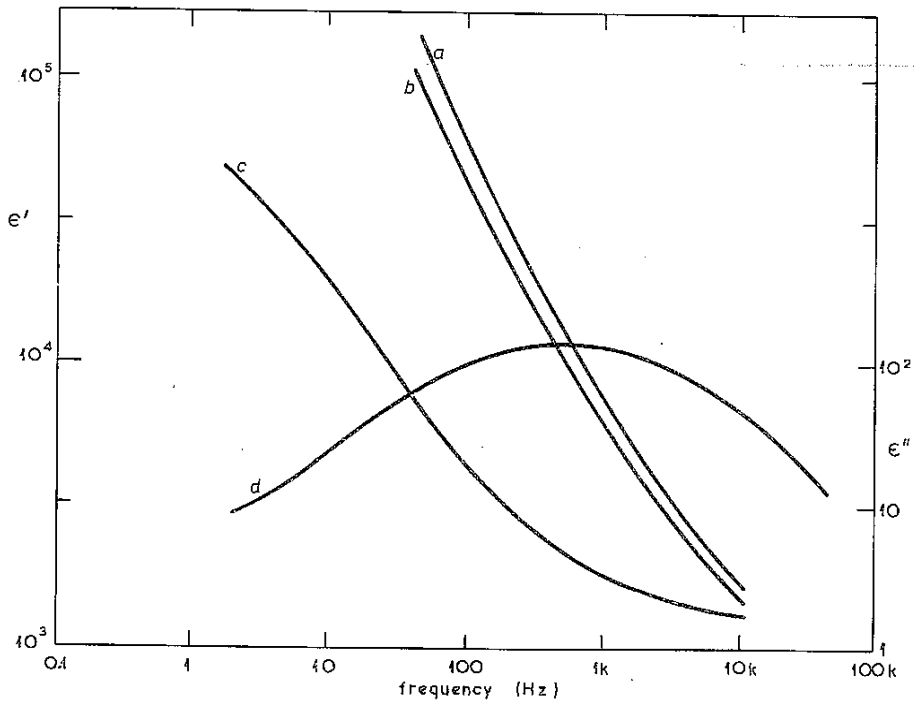

Fig. 16 In vivo *dielectric spectra for normal legs (a) Left calf; (b) Right calf; (c) Knee; (d) Knee*

dielectric properties of such tissues did not correspond with the *in vivo* properties of these tissues, but usually those of the preservative fluid, which was formalin in the most part. This is the reason that the results on such tissues were so similar.

Many of the measurements were repeated. It is now possible to obtain 'normal' curves for dielectric measurements on healthy tissues. Fig. 12 shows some of these; curves *a* and *b* are the measurements on a 'normal' arm.

In order to obtain consistent results, care must be taken to clean the skin thoroughly with surgical spirit and then dry it carefully before sticking on the jelly electrodes. Curve *c* was obtained after occlusion of the same arm. The overlap between curves *a* and *b* is good, while curve *c* shows many slight variations from the other curves, especially at low frequencies.

Fig. 13 represents the results of *in vitro* measurements on human blood samples. Fresh venous blood was obtained from a volunteer (BS) and heparinised. A measurement cell was constructed in a hypodermic syringe using silver-mesh electrodes. The blood was kept at the room temperature (21°C) and the results of this measurement are represented by curve *a* in Fig. 13.

This curve is similar to those obtained by CHELIDZE *et al.* (1973*a*, *b*). Curves *b* and *c* in the same Figures show the results of measurements on r.b.c. rich blood (after two hours of centrifuging at 2000 r/min and on clotted blood, respectively.

If the curves *a* and *b* in Fig. 13 had followed the dotted line, they would have satisfied the Debye relaxation theory. The suggested membrane theories of FRICKE (1925) and PAULY and SCHWAN (1959), whereby a dispersion is described on the basis of a membrane capacitance C_m and a membrane conductivity C_m may not be applicable to measurements on blood. The present results on blood were obtained to estimate the potentialities of the instrument and therefore the variables were not under close control. It would be premature to suggest any mechanism on the evidence of these results. The presence of two time constants in the Debye lumped circuit gives rise to two distinct peaks (curve *a*, Fig. 14) at the two characteristic frequencies. The simulated sample had the two time constants ($T = 1/\omega$) 10^{-3} and 10^{-5}. Curve *b* in the same Fig. 14 was obtained by measuring a piece of excised fatty tissue from a female breast and this also shows two dispersion peaks.

Some very interesting results were obtained from 'normal' female breasts compared with those having tumours. In Fig. 15, curves *a* and *b* were obtained from the normal breasts of two different patients, and, apart from a small displacement, the two curves are very similar. Curves *c* and *d* are the results of measurements on breasts which contained tumours. Curve *d* corresponds with what was subsequently found on section to be a benign tumour, and curve *c* to be a malignant tumour. This last result (breast

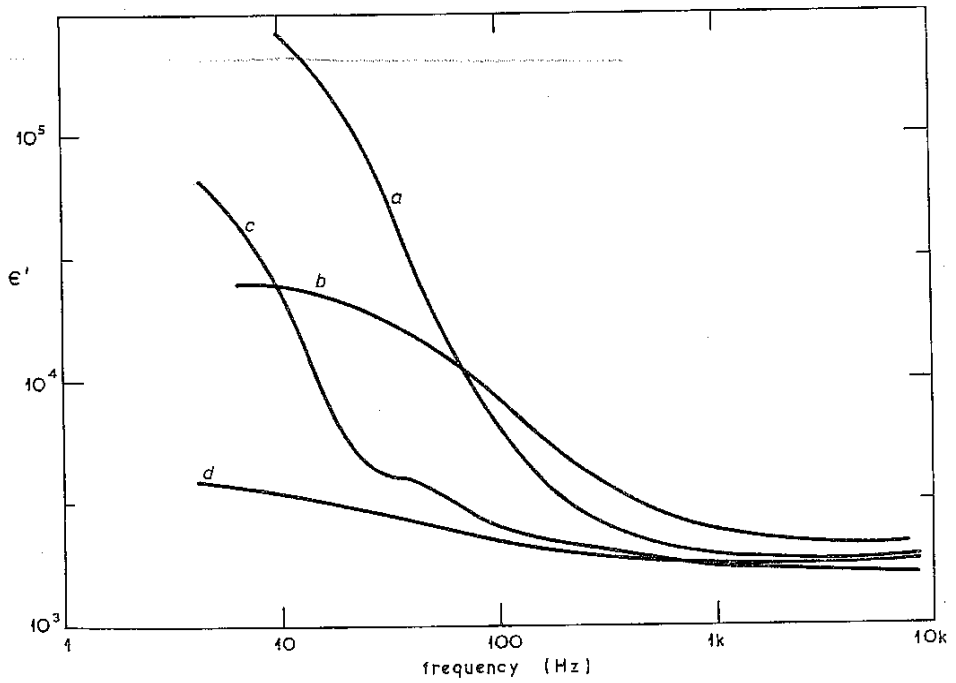

Fig. 17 In vivo *dielectric spectra (a) Normal breast, external electrode (b) Palm, external electrodes (c) Biceps, external electrodes (d) Normal breast, hypodermic electrodes*

tumour with malignancy) was repeated with hypodermic needles inserted beneath the skin. The numerical results thus obtained are different because with the internal electrodes it was not possible to obtain absolute values of the relative permittivity and dielectric loss because of the shape of the electrodes used. However, the dielectric constant in this case is lower in value than that obtained with external electrodes (curve *e*).

Figs. 16–19 show the results of measurement on a wide range of different tissues. The differences are most pronounced when tissues which include bones are compared with those which do not include any bones.

7 Conclusions

A new technique for the measurement of dielectric constant of body-tissues *in vivo* has been described, together with an instrument which rapidly measures the complex dielectric constant over a range of frequencies from 0·1 Hz to 100 kHz if full use is made of the resolution of the data points collected and stored in the r.a.m.

The minimum change of the relative permittivity that can be resolved with this instrument corresponds to 1: 25 000 of the value of the reference capacitor at the input of the amplifier, and the accuracy of measurement is limited by digitisation to ± 3%. The instrument has been used on a single time constant Debye lumped circuit and on biological materials of different descriptions.

From the preliminary results obtained with the equipment, it is clear that different tissues have different dielectric properties in this frequency range to an extent which could have clinical applications. The materials examined so far have been used mainly to develop the equipment to a point where apparently meaningful biological variations can be detected. It is now possible for a clinician to operate the equipment after a brief explanation and the technique is quite acceptable to the patients even when internal electrodes are used.

A parallel investigation of the dielectric properties of tissues was undertaken at Wigan Infirmary using breast tumours as a convenient system (Fig. 11). The female breast has the advantage of a relatively simple and uniform cellular structure with a conveniently symmetrical normal organ present in most cases. Results such as those shown in Fig. 11 were obtained using a constant current source and measuring the tissue impedance at discrete frequencies. They also show differences which suggest that

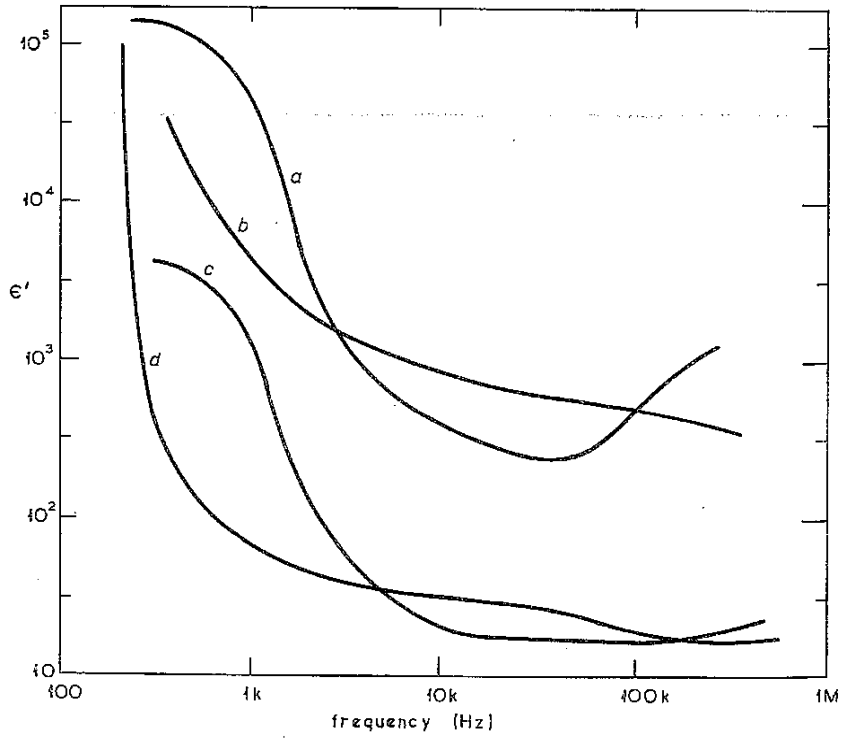

Fig. 18 In vivo *dielectric spectra using the electrodes shown in Fig. 9. (a) Thumb (b) Thigh (c) Wrist (d) Ankle*

useful clinical information about a breast tumour might be obtained with the equipment described in this paper. Because of the greater rapidity of measurement using the dielectric spectrometer, many more patients could be measured rapidly. It is intended to continue this clinical evaluation as a priority.

Several other fields of possible clinical application have been suggested (MARKOVICH, 1970; CLYNES and MILSUM, 1970). The possibility of detecting small changes in the cell/extracellular fluid ratio

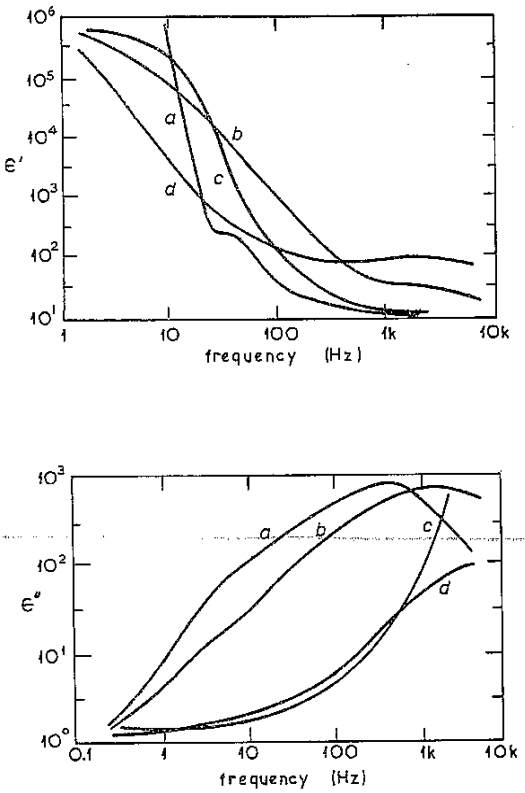

Fig. 19 In vitro *dielectric spectra for fresh excised tissues: (a) Rib (b) Trachea (c) Liver (d) Kidney*

(Fig. 13) could be used to detect conditions in which mild degrees of oedema may be the first significant change, e.g. deep-vein thrombosis and early oedema of the brain in neonates. More gross changes such as intracranial or intracerebral bleeding might be detected by this apparatus and provide a simpler, cheaper and more rapidly available technique than the present methods used for these conditions. These and other possibilities can now be checked by short pilot studies on patients.

Acknowledgments—The authors gratefully acknowledge the very useful assistance rendered by J. S. S. Stewart, surgeon of the Wigan Infirmary, in providing the clinical facilities for testing the instrument. Acknowledgments are also due to R. M. Winston, Consultant Pathologist, Hope Hospital, Salford, for calling attention to the paper by FRICKE and MORSE (1926) and to D. E. Clark, Director, Medical Computing Unit, University of Manchester, for facilities for trying this instrument on his computing packages. Finally, the authors are indebted to the UK Science Research Council, for providing the research grant in support of this work (Ref. No. B/RG/4354.5).

References

CHELIDZE, T. L., KIKNADZE, V. D., KEVLISHVILI, F. Ye and CHKHAIDZE, V. T. (1973*a*) Dielectric spectroscopy of blood II. *Biofizika* **18**, 868–872.

CHELIDZE, T. L., KIKNADZE, V. D., KEVLISHVILI, F. Ye. and CHKHAIDZE, V. T. (1973*b*) Dielectric spectra of normal human blood. *ibid.* **18**, 932–935.

CLYNES, M. and MILSUM, J. H. (Eds.) (1970) Electrical impedance cephalography. In *Biomedical engineering systems*, McGraw-Hill, London, 21–64.

FRICKE, H. and MORSE, S. (1926) The electric capacity of tumors of the breast. *J. Cancer Res.* **10**, 340–376.

DELAHAY, P. (1954) *New instrumental methods in electrochemistry*, Interscience, Chichester.

FRICKE, H. (1925) A mathematical treatment of the electric conductivity and capacity of disperse systems. *Phys. Rev.* **26**, 678–681.

HYDE, P. J. (1970) Wide-frequency-range dielectric spectrometer. *Proc. IEE* **117**, 1891–1901.

KOLTHOLF, I. M. and LINGANE, J. J. (1952) *Polarography* —Vol. 1, John Wiley, New York.

MARKOVICH, S. E. (Ed.) (1970) International conference on bioelectric impedance. *Ann. New York Acad. Sci.* **170**, Art 2, 407–836.

PAULY, H. and SCHWAN, H. P. (1959) Über die Impedanz einer suspension von Kugelförmigen Teilchen mit einer Schale. *Z. Naturforsuch.* **14b**, 125–131.

VAN DER PAUW, L. J. (1958) A method of measuring specific resistivity and Hall effect of discs of arbitrary shape. *Philips Res. Repts.* **13**, 1–9.

SCHWAN, H. P. (1957) Electrical properties of tissue and cell suspensions. *Adv. Biol. Med. Phys.* **5**, 147–209.